AIMS Materials Science, 4(3): 540-550.
DOI: 10.3934/matersci.2017.3.540
Received: 15 December 2016
Accepted: 05 March 2017
Published: 06 April 2017

http://www.aimspress.com/journal/Materials

Research article

Supercritical hydrothermal synthesis of polycrystalline gadolinium aluminum perovskite materials ($GdAlO_3$, GAP)

HN Girish [1,2,*], P Madhusudan [1,2], CP Sajan [3], BV Suresh Kumar [1], and K Byrappa [1]

[1] Department of Studies in Earth Science, University of Mysore, Mysore 570 006, India
[2] State Key Laboratory of Advanced Technology for Materials Synthesis and Processing, Wuhan University of Technology, Wuhan 430070, China
[3] Department of Environmental Science, University of Mysore, Mysore 570 006, India

* **Correspondence:** Email: girishhn25@gmail.com; Tel: +91-9036358072.

Abstract: The orthorhombic perovskite, Gadolinium aluminum oxide ($GdAlO_3$, GAP) material was successfully prepared by hydrothermal supercritical fluid method using co-precipitated gel of GAP. All experiments were carried out in the pressure and temperature ranges of 100–150 MPa and 180–650 °C respectively. The as-prepared GAP samples were systematically characterized by X-ray diffraction (XRD), scanning electron microscopy (SEM), Fourier transform infrared spectroscopy (FT-IR), X-ray spectroscopy (EDS), thermo gravimetry (TGA) and differential thermo gravimetry analysis (DTA). The XRD profile confirms fully crystalline and orthorhombic nature of as-prepared materials, which is well correlated to the reported results. The SEM studies reveal that the GAP materials synthesized at 650 °C/150 MPa for 92 hrs possesses polycrystalline nature with average particle size in the range of 5–20 μm. The DTA shows a crystallization peak at 361 °C at this temperature the agglomerated GAP gel starts to crystallize into polycrystalline GAP materials. When compared with other methods, like sol-gel and solid-state reactions our crystallization temperature is very much lower and feasible. This work not only demonstrates a simple way to fabricate GAP polycrystalline materials from co-precipitated gels but also shows a possible utilization of same technique for synthesis of other high temperature materials.

Keywords: co-precipitated gel; hydrothermal process; perovskite; supercritical temperature

1. Introduction

Ceramic based materials on the Ln_2O_3-Al_2O_3 system (Ln-Lanthanide element) have shown their potential applications as a neutron absorber, flux suppressors, and high-temperature container materials [1]. Further, processing of these materials is considerable interest due to their magnetic and optical properties [1–4]. The study of rare-earth perovskite is of huge interest because of their relatively simple crystal structure with many diverse electric, magnetic, optical, piezoelectric, catalytic, and magnetoresistive properties. Among aluminum perovskite group, several of them are employed has host for solid state-state laser, luminescence system, solid electrolytes, chemical sensors, magnetic refrigeration materials, substrates for high-temperature superconductor deposition, catalyst supports and thermal barrier coatings [5,6]. Gadolinium aluminum perovskite (GAP) are widely used in the preparation of phosphors for color TV tubes [7–11], scintillator [12], regenerator material for sub-4k cryo-coolers [13], Luminescence thermometry with Eu^{3+} doped GAP [14], as well as a potential host system for materials with oxygen ion conductivity [15,16,17]. Currently, GAP material is under development as a candidate for the neutron absorption and control rod applications. Conventionally, GAP is produced by solid-state reaction of gadolina and alumina powder which involves extensive mechanical mixing followed by heat treatment for prolong duration and sintering at relatively high temperatures (1650–1700 °C) [18,19]. To avoid the problem associated with solid-state synthesis of GAP powder, several wet-chemical techniques, such as polymerized complex route, combustion system, sol-gel, flux methods, melt technique, citrate-nitrate solution and microwave technique have been used to synthesize GAP [7,9,15,20–27]. However, these are high-temperature methods which consume a lot of energy and lead to certain thermally induced strain in the resultant products thereby affecting their quality and indorsing crystal defects. In our previous investigation, we reported the synthesis of the pure phase of aluminum perovskite materials using supercritical hydrothermal technique [28,29,30]. The supercritical hydrothermal technique (SHT) has advantages over mild hydrothermal technique (MHT) to obtain $GdAlO_3$ powder with high purity and homogeneity, fine crystallinity, narrow size distribution and controlled particle morphology. Beyond the supercritical point (373.946 °C/22.064 MPa) in the liquid–vapor space, water exists as small but liquid-like (associated) hydrogen-bonded clusters dispersed within a gas-like (dissociated) phase [31]. Previously, we had investigated hydrothermal synthesis of GAP particles with significance to their phase formation [32]. In this paper, we extend our previous research work and have varied the experimental environments and discussed about the favorable condition employed for synthesis of orthorhombic GAP phase. Our preparation conditions are much milder and simpler than those of conventional solid-state method, which require high-temperature heat treatment. Further, the TG-DSC behavior of co-precipitated gel during the formation of GAP polycrystalline phase has been discussed. The SEM images of as-prepared GAP materials are compared and discussed with co-precipitated GAP gel starting materials. The particle size and morphology of the GAP materials synthesized at 650 °C/150 MPa are quite different from our previously reported results. The as-prepared samples were subjected to systematic characterization using thermal analysis/differential scanning calorimetry (TG/DSC), powder X-ray diffraction (XRD), Fourier transform infrared spectroscopy (FTIR), scanning electron microscope and energy dispersive X-ray spectroscopy (SEM/EDAX).

2. Materials and Method

2.1. Materials

Gadolinium oxide (LOBA Chemie Co. Ltd, purity 99.9%, extra pure), aluminum oxide (LOBA Chemie Co. Ltd., purity 99%, neutral), nitric acid (LOBA Chemie Co. Ltd., purity 69%, pure), ammonium solution (LOBA Chemie Co. Ltd.). All the reagents were of analytical grade and used without further purification. Deionized water was used for post treatment processes.

2.2. Hydrothermal Synthesis of Gadolinium Aluminum Perovskite ($GdAlO_3$, GAP)

Synthesis of gadolinium aluminate ($GdAlO_3$, GAP) polycrystalline ceramics materials by hydrothermal supercritical technique were carried out using externally heated (Tuttle-Roy test tube type) pressure vessels. The co-precipitated gels of gadolinium and aluminum were used as precursors. These co-precipitate gels are more sensitive and highly reactive materials for the synthesis of perovskite materials. The possible reaction mechanism for the formation of GAP co-precipitate gel is as shown:

$$Gd_2O_3 + 6HNO_3 \rightarrow 2Gd(NO_3)_3 + 3H_2O \quad (1)$$

$$Al_2O_3 + 6HNO_3 \rightarrow 2Al(NO_3)_3 + H_2O \quad (2)$$

$$Gd(NO_3)_3 + Al(NO_3)_3 + 6NH_4OH \rightarrow Gd(OH)_3 + Al(OH)_3 + 6NH_4NO_3 \quad (3)$$

$$Gd(OH)_3 + Al(OH)_3 \rightarrow 1/2Gd_2O_3 + 1/2Al_2O_3 + 3H_2O \quad (4)$$

$$1/2Gd_2O_3 + 1/2Al_2O_3 \rightarrow GdAlO_3 \quad (5)$$

The schematic flow chart for the preparation of co-precipitation gel using respective raw materials is illustrated in Figure 1. Similar, method was also adopted by Basavalingu *et al*. for the synthesis of orthorhombic $YAlO_3$ [28] and, Hamilton & Henderson for preparation of silicate minerals [33]. The experimental details of hydrothermal runs on the synthesis of GAP materials are shown in Table 1. The experiments were carried out using the conventional test tube type Tuttle-Roy externally heated pressure vessels in the pressure and temperature range of 100–150 MPa and 180–650 °C, respectively. The starting co-precipitated gels were homogeneously mixed and were taken in a sealed gold tube of 50–60 mm in length and 4.5 mm in outer diameter and with wall thickness of 0.1 mm. The capsules were carefully sealed with arc welding after taking the appropriate quantity of starting charge comprising of both solids and liquids. The capsules were checked for leakage before placing into the vessel by keeping them for extended heating in a hot air oven at 100 °C for check any weight difference. The capsules showing any weight loss during this process were discarded. The duration of the experimental runs was 48 to 92 hours, and later the vessels were quenched by compressed air blast. After the desired experimental condition the run products was carefully removed by cutting the capsules, was recovered, washed with distilled water, ultrasonicated and dried in hot air oven at 70 °C for 8 hours. The resultant product obtained was subjected to further characterization using different analytical techniques.

2.3. Material Characterization

The reaction process was studied by using differential scanning calorimetry and thermogravimetric

analyses (DSC-TG, Netzsch STA 449F3, Germany) for prepared co-precipitated gel from RT (room temperature) to 1400 °C. The XRD analysis was carried out to study the crystalline phase at ambient temperature using Rigaku-D/MAX-2400 diffractometer with CuKα radiation from $2\theta = 0°$ to 70° at a step of 0.05°. The infrared spectra in the range of 4000–400 cm^{-1} were recorded using FT-IR spectrophotometer, Jasco 460 plus, Japan. Energy dispersive X-ray analyses (EDAX) were used for quantitative analysis and scanning electron microscope (SEM) model JEOL JSM-6380LA was used for studying the morphology and microstructure of the as-prepared samples.

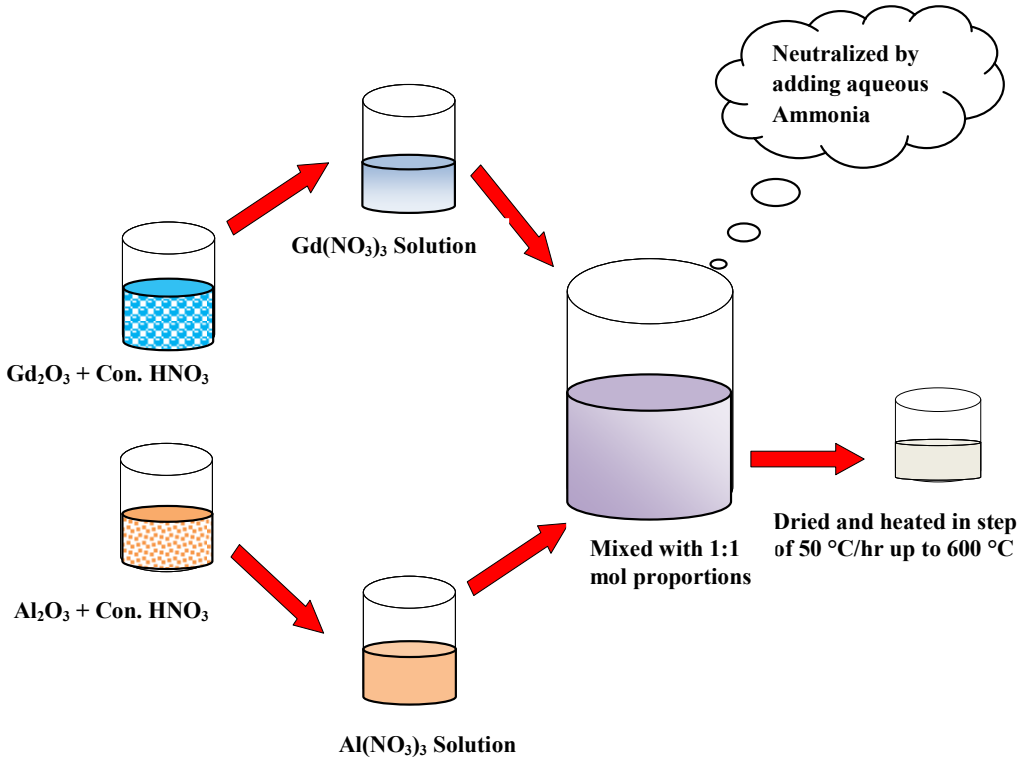

Figure 1. Schematic diagram have different steps for preparation of GAP co-precipitated gel.

3. Results and Discussion

3.1. TG-DSC Curve Analysis of Co-precipitate Gel

The thermogravimetric and differential thermal analysis of co-precipitated gel were carried out using a Netzsch STA 449F3, Germany in the temperature range 20–1400 °C at a heating rate of 10 °C/min under Argon atmosphere and the results are illustrated in Figure 2. The TG-DSC profile clearly depicts that during the preparation of co-precipitate gel which involves different step like aging, drying, and heating at 600 °C, H_2O and volatile compound like NH_3 were released. It was also observed that there was a small endothermic reaction at 75.6 °C which is attributed to the release of a trace amount of moisture and NH_3 gas. Further, major weight loss was observed at the temperature range between 300–400 °C. This is due to the evolution of gasses such as NO, NH_3, and NO_2. The DTA shows a crystallization peak at 361 °C at this temperature the agglomerated GAP gel starts to crystallize into polycrystalline GAP materials. At the region of 1148 °C, a small exothermic peak was observed

which is associated with significant weight change in the sample complete formation of orthorhombic GAP. The crystallization temperature is lower when compared to other methods, like solid-state reactions [19].

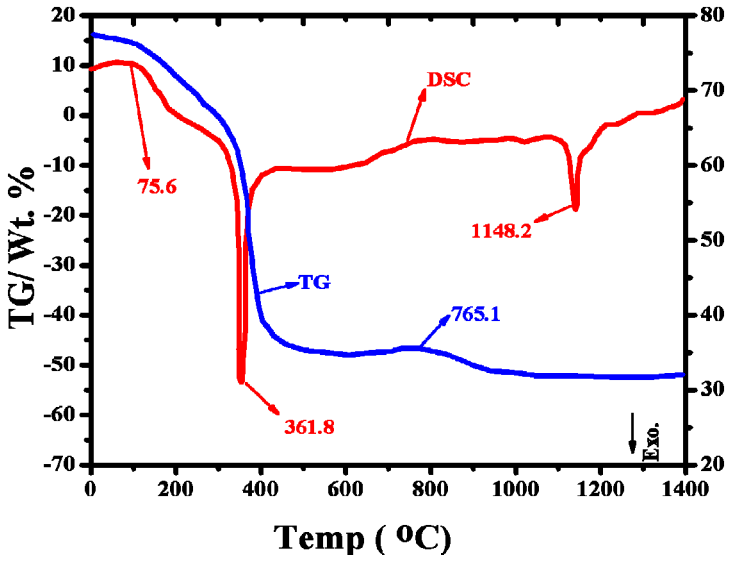

Figure 2. TG and DSC profile curves of precursor sample recorded from ambient to 1400 °C with a heating rate of 10 °C/min under Argon atmosphere.

Table 1. Experimental detail for the synthesis of GAP in different experimental condition (CPG = Co-precipitated gel).

Exp. No.	Precursors	Temp. (°C)	Pressure (MPa)	Duration (hrs.)	Run Product
HN-6	$Gd_2O_3 + Al_2O_3 + H_2O$	180	autonomous	72	$Gd_2O_3 + Al_2O_3$ powder
HN-10	$Gd_2O_3 + Al_2O_3 + H_2O$	200	autonomous	48	$Gd_2O_3 + Al_2O_3$ powder
HN-12	$Gd_2O_3 + Al_2O_3 + H_2O$	200	autonomous	72	$Gd_2O_3 + Al_2O_3$ powder
HN-16	CPG + H_2O	200	autonomous	72	Al_2O_3 powder
HN-21	CPG + H_2O	400	autonomous	72	Al_2O_3 powder
HN-25	CPG + H_2O	400	100	48	$Gd_2O_3 + Al_2O_3$ mix phase
HN-31	CPG + H_2O	500	100	48	$Gd_2O_3 + Al_2O_3$ mix phase
HN-37	CPG + H_2O	500	100	72	$Gd_2O_3 + Al_2O_3$ mix phase
HN-39	CPG + H_2O	600	120	72	GAP + Al_2O_3 phase
HN-41	CPG + H_2O	600	120	92	GAP + Al_2O_3 phase
HN-47	CPG + H_2O	650	150	92	GAP phase
HN-49	CPG + H_2O	650	150	92	GAP phase

3.2. X-ray Diffraction

The XRD patterns of the co-precipitated gel, synthesized GAP and reported GAP standard material are shown in Figure 3. The XRD pattern of co-precipitated gel used as the starting material for GAP synthesis was amorphous in nature without any diffraction peaks. On the other hand, the XRD pattern of

as-prepared GAP polycrystalline materials matches well with already reported PDF, 46-0395 of orthorhombic $GdAlO_3$ phase [34]. The peaks in the region 23.87, 33.98, 42.08, 48.77, 55.09 and 60.98 corresponds to (002), (112), (202), (220), (114) and (312) planes, respectively. The resultant X-ray pattern is similar to the X-ray diffraction data of GAP synthesized by solution combustion method [10,24], sol-gel method where the samples were repeatedly dried and sintered at 1000 °C for 10 hrs [35], nanocrystalline $GdAlO_3$ synthesized in citrate gel method in absence of oxygen at 1200 °C [23], reverse micelle method where calculations was carried at temperature above 1000 °C [36], synthesized Eu^{3+} doped $GdAlO_3$ in solid state reaction above 1000 °C [19] and Tb^{3+} and Bi^{3+} doped $GdAlO_3$ synthesized by solvothermal reaction method at 1000 °C [8]. It was observed that at a temperature less than 600 °C, and 150 MPa pressure, the resultant products were a mixed phase and the small peak arise at 23.8 theta region matches with Al_2O_3 impurity phase (not shown). The refinement of lattice parameters was done using CHEKCELL software and obtained lattice parameters was compared with the reported data which is shown in Table 2. From the XRD pattern of the GAP, it is clear that the synthesized compound possess highly crystallized pure phase. The cell parameter of the synthesized GAP is different in a small amount which might be due to the experimental conditions.

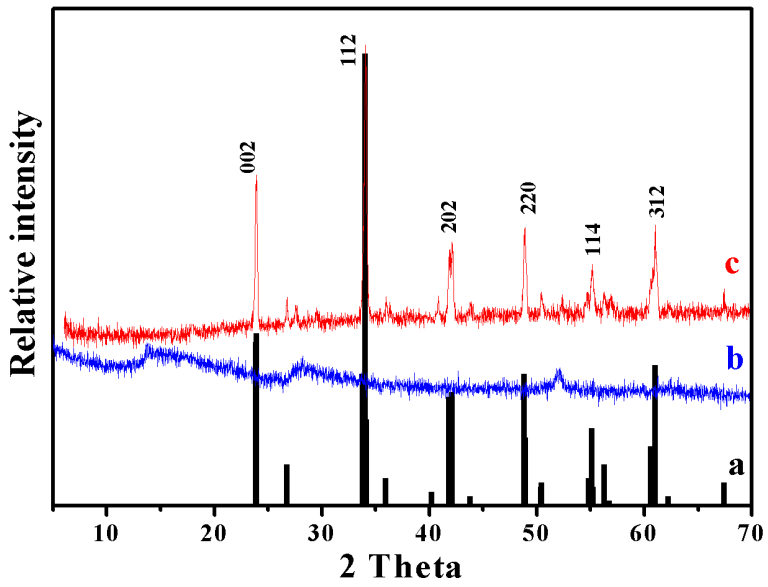

Figure 3. X-ray diffraction pattern: a) reported a pattern of GAP, JCPDS = 46-0395 [34], b) Co-precipitated gel of GAP and c) Synthesized GAP at 650 °C/150 MPa at 92 hrs.

Table 2. Refined lattice parameters of synthesized GAP compared with reported data.

Compound	*a*-axis (Å)	*b*-axis (Å)	*c*-axis (Å)	Cell volume (Å^3)
GAP (PDF = 46-0395) [34]	5.251	5.301	7.445	207.27
Synthesized GAP	5.243	5.302	7.441	207.12

3.3. Infrared Spectra and SEM with EDAX Analysis

To investigate the chemical composition and chemical bonding of co-precipitate gel of GAP and polycrystalline GAP materials, FT-IR was carried out and the corresponding spectra are shown in

Figure 4. In the FT-IR spectrum of the co-precipitate gel (Figure 4a), there is a broad strong absorption at around 3450 cm^{-1} and a narrow band at 1635 cm^{-1} which are assigned to the stretching and bending modes of absorbed water, respectively. Figure 4b presents FT-IR spectra of the GAP sample synthesized at 650 °C/150 MPa condition. The small absorption band from 3000 cm^{-1} to 3800 cm^{-1} corresponds to the OH mode which might be due to the water molecules absorbed at room temperature. On the other hand, –C=C– bond in the synthesized GAP material is represented by the band at 1570 cm^{-1} which might be due to the adsorption of atmospheric carbon (Figure 4b). The band appearing at 1381 cm^{-1} corresponds to vibration modes of NO_3 groups. The band observed in the low-frequency region of the spectrum, corresponds to the lattice vibration mode which is attributed to typical gadolinium oxygen (Gd–O) vibration at 520 cm^{-1}. The band frequencies at 660 and 465 cm^{-1} which are typical of the Al–O stretching characteristic vibrations in the perovskite structure compounds [37–40].

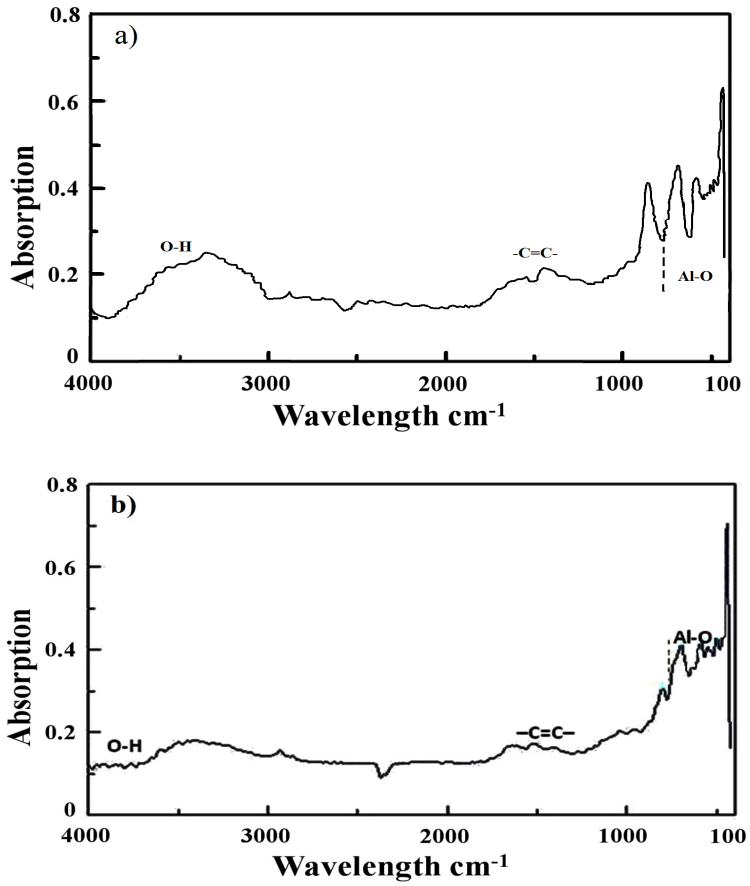

Figure 4. FT-IR spectrum: a) Co-precipitate gel of GAP at room temperature, b) Synthesized GAP at 650 °C/150 MPa at 92 hrs.

The morphology and the particle size of the resultant product were analyzed by SEM. The SEM images of the prepared co-precipitate gel were agglomerate in nature (Figure 5a and 5b) which is in agreement with the XRD result which showed amorphous nature. The SEM image of GAP materials synthesized at 650 °C/150 MPa for 92 hrs possesses polycrystalline nature with the orthorhombic crystal structure (Figure 5c and 5d). The SEM images further reveal that the average particle size of synthesized GAP crystals is in a range of 5–20 μm, which clearly shows that are as-prepared products are

homogeneous material with polycrystalline nature. Furthermore, it is worth to reveal that the morphology of our synthesized GAP material is quite difference than $GdAlO_3$ synthesized from sol-gel technique [22] and our previous results [32]. Based on XRD and SEM studies it was conformed that the phase formation under hydrothermal supercritical condition mainly depends on the nature of precursor materials, crystallization temperature and pressure. The atomic percentage of elements present in the as-prepared sample was performed at magnification 200× high voltage of 15.0 kV. The atomic percentage of elements, i.e, Gd, Al and O present in the sample is shown in Table 3. From the EDAX analysis, it is clear that the synthesized sample is free from impurities and doesn't contain any foreign materials. Furthermore, the morphological study in support with compositional study confirms that these crystals possess nominal phase stoichiometry and the supercritical fluids generated inside the gold capsules has greatly influenced in the resultant morphology of the crystals and also maintain their chemical composition.

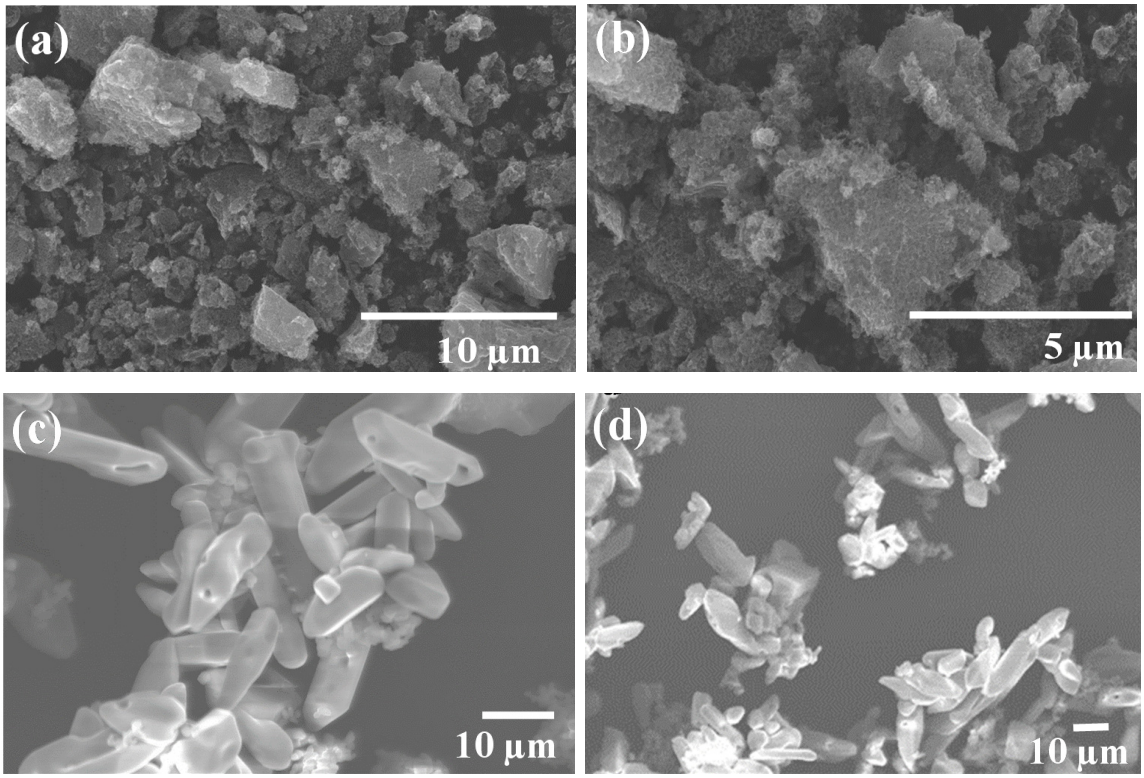

Figure 5. SEM images: a & b) as prepared Co-precipitate gel of GAP; c & d) synthesized GAP at 650 °C/150 MPa for 92 hrs.

Table 3. Percentage composition of GAP.

Run product	O (at.%)	Al (at.%)	Gd (at.%)	Total (at.%)
GAP	20.72	25.56	53.72	100

4. Conclusions

In summary, we have reported the synthesis of polycrystalline GAP materials under the influence

on supercritical hydrothermal fluid condition. The composition of the starting charge materials and experimental condition play an important role in preparation of GAP crystals. So far it was difficult to synthesize single phase GAP materials due to their difficulty in controlling stoichiometric composition. In this paper, we have conducted the experiments at pressure and temperature ranges of 100–150 MPa and 180–650 °C respectively. Further, the as-prepared GAP samples were systematically characterized by different analytical techniques. The XRD results of samples prepared at 650 °C/150 MPa shows well crystalline orthorhombic phase and SEM shows the samples are of 5–20 μm in size. The synthesis temperature of our experiments was lower than other methods, like sol-gel and solid-state reactions. The current strategy not only demonstrates a simple possible way to fabricate the orthorhombic phase of GAP polycrystalline material from co-precipitated gel, but also shows a prospect for further investigations on the synthesis of similar rare-earth doped oxides for customized applications.

Conflict of Interest

The authors declare that there is no conflict of interest.

References

1. Attfield JP (2001) Structure–property relations in doped perovskite oxides. *Int J Inorg Mater* 3: 1147–1152.
2. Atwood DA, Yearwood BC (2000) The future of aluminium chemistry. *J Organomet Chem* 600: 186–197.
3. Cashion JD, Cooke AH, Hawkes JFB, et al. (1968) Magnetic Properties of Antiferromagnetic $GdAlO_3$. *J Appl Phys* 39: 1360–1361.
4. Cashion JD, Cooke AH, Leask MJM, et al. (1968) Crystal Growth and Magnetic Susceptibility of Some Rare-Earth Compounds. Part 2. Magnetic Susceptibility Measurements on a Number of Rare-Earth Compound. *J Mater Sci* 3: 402–407.
5. Vonka P (2009) A method for the estimation of the enthalpy of formation of mixed oxides in Al_2O_3-Ln_2O_3 systems. *J Solid State Chem* 182: 744–748.
6. Hayashi H, Inaba H, Matsuyama M, et al. (1999) Structural consideration on the ionic conductivity of perovskite-type oxides. *Solid State Ionics* 122: 1–15.
7. Han SD, Khatkar SP, Taxak VB, et al. (2006) Combustion synthesis and luminescent properties of Eu^{3+}-doped $LnAlO_3$ (Ln = Y and Gd) phosphors. *Mater Sci Eng B* 127: 272–275.
8. Park JY, Jung HC, Raju GSR, et al. (2010) Enhanced green emission from Tb^{3+}–Bi^{3+} co-doped $GdAlO_3$ nanophosphors. *Mater Res Bull* 45: 572–575.
9. Oliveira HHS, Cebim MA, Da Silva AA, et al. (2009) Structural and optical properties of $GdAlO_3$:RE^{3+} (RE = Eu or Tb) prepared by the Pechini method for application as X-ray phosphors. *J Alloy Compd* 488: 619–623.
10. Jisha PK, Naik R, Prashantha SC, et al. (2015) Facile combustion synthesized orthorhombic $GdAlO_3$:Eu^{3+} nanophosphors: Structural and photoluminescence properties for WLEDs. *J Lumin* 163: 47–54.
11. Selvalakshmi T, Venkatesan P, Wu SP, et al. (2017) Gd_2O_3:RE^{3+} and $GdAlO_3$:RE^{3+} (RE = Eu, Dy) Phosphor: Synthesis, Characterization and Bioimaging Application. *J Nanosci Nanotechno* 17: 1178–1184.

12. Verweij JWM, Cohen-Adad MT, Bouttet D, et al. (1995) Luminescence properties of $GdAlO_3$:Ce powders. Dependence on reduction conditions. *Chem Phys Lett* 239: 51–55.
13. Qiu LM, Numazawa T, Thummes G (2001) Performance improvement of a pulse tube cooler below 4 K by use of $GdAlO_3$ regenerator material. *Cryogenics* 41: 693–696.
14. Lojpur V, Ćulubrk S, Medić M, et al. (2016) Luminescence thermometry with Eu^{3+} doped $GdAlO_3$. *J Lumin* 170: 467–471.
15. Sinha A, Sharma BP, Gopalan P (2006) Development of novel perovskite based oxide ion conductor. *Electrochim Acta* 51: 1184–1193.
16. Sinha A, Näfe H, Sharma BP, et al. (2008) Study on Ionic and Electronic Transport Properties of Calcium-Doped $GdAlO_3$. *J Electrochem Soc* 155: B309–B314.
17. Luo H, Bos AJJ, Dorenbos P (2016) Controlled Electron–Hole Trapping and Detrapping Process in $GdAlO_3$ by Valence Band Engineering. *J Phys Chem C* 120: 5916–5925.
18. Cao G (2004) *Nanostructures and Nanomaterials: Synthesis, Properties and Applications*, London: Imperial College Press.
19. Upadhyay K, Tamrakar RK, Dubey V (2015) High temperature solid state synthesis and photoluminescence behavior of Eu^{3+} doped $GdAlO_3$ nanophosphor. *Superlattice Microst* 78: 116–124.
20. Raju GSR, Park JY, Jung HC, et al. (2009) Synthesis and luminescent properties of low concentration Dy^{3+}:GAP nanophosphors. *Opt Mater* 31: 1210–1214.
21. Gao H, Wang Y (2007) Preparation of (Gd, Y)AlO_3:Eu^{3+} by citric-gel method and their photoluminescence under VUV excitation. *J Lumin* 122–123: 997–999.
22. Cizauskaite S, Reichlova V, Nertavicience G, et al. (2007) Sol-gel preparation and characterization of perovskite gadolinium aluminates. *Mater Sci-Poland* 25: 755–765.
23. Sinha A, Sharma BP, Näfe H, et al. (2010) Synthesis of gadolinium aluminate powder through citrate gel route. *J Alloy Compd* 502: 396–400.
24. Sinha A, Nair SR, Sinha PK (2011) Single step synthesis of $GdAlO_3$ powder. *J Alloy Compd* 509: 4774–4780.
25. Catunda T, Andreeta JP, Castro JC (1986) Differential interferometric technique for the measurement of the nonlinear index of refraction of ruby and $GdAlO_3$:Cr^{+3}. *Appl Optics* 25: 2391–2395.
26. Harada Y, Uekawa N, Kojima T, et al. (2009) Fabrication of dense material having homogeneous $GdAlO_3$-Al_2O_3 eutectic-like microstructure with off-eutectic composition by consolidation of the amorphous. *J Eur Ceram Soc* 29: 2419–2422.
27. Selvam MP, Rao KJ (2000) Microwave synthesis and consolidation of gadolinium aluminum perovskite, a ceramic extraordinaire. *Adv Mater* 12: 1621–1624.
28. Basavalingu B, Girish HN, Byrappa K, et al. (2008) Hydrothermal synthesis and characterization of orthorhombic yttrium aluminum perovskites (YAP). *Mater Chem Phys* 112: 723–725.
29. Girish HN, Vijayakumar MS, Devaraju MK, et al. (2009) Hydrothermal Synthesis and Characterization of Neodymium doped Yttrium Aluminum Perovskite (Nd:YAP). *Indian Mineral* 43: 162–168.
30. Basavalingu B, Kumar MSV, Girish HN, et al. (2013) Hydrothermal synthesis and characterization of rare earth doped yttrium aluminium perovskite—R:$YAlO_3$ (R = Nd, Eu & Er). *J Alloy Compd* 552: 382–386.

31. Rukes B, Dooley RB (2001) Guideline on the Use of Fundamental Physical Constants and Basic Constants of Water. International Association for the Properties of Water and Steam, Gaithersburg, Maryland, USA, 1–7.
32. Girish HN, Basavalingu B, Shao GQ, et al. (2015) Hydrothermal synthesis and characterization of polycrystalline gadolinium aluminum perovskite ($GdAlO_3$, GAP). *Mater Sci-Poland* 33: 301–305
33. Hamilton DL, Henderson CMB (1968) The preparation of silicate compositions by a gelling method. *Mineral Mag* 36: 832–838.
34. Wang P (1994) Shanghai Inst. of Ceramics, Chinese Academy of Science, Shanghai, China.
35. Cizauskaitė S, Špakauskaitė G, Beganskienė A, et al. (2006) A comparative study of $GdAlO_3$ perovskite prepared by the sol-gel method using different complexing agents. *Chemija* 17: 40–45.
36. Chandradass J, Kim KH (2010) Reverse Micelle-Directed Synthesis of $GdAlO_3$ Nanopowders. *Mater Manuf Process* 25: 1428–1431.
37. Schrader B (1995) *Infrared and Raman Spectroscopy, Method and Application*.
38. Nakamoto K (1986) *Infrared and Raman Spectroscopy of Inorganic and Coordination Compounds*.
39. Vaqueiro P, López-quintela MA (1998) Synthesis of yttrium aluminium garnet by the citrate gel process. *J Mater Chem* 8: 161–163.
40. Chroma M, Pinkas J, Pakutinskiene I, et al. (2005) Processing and characterization of sol-gel fabricated mixed metal aluminates. *Ceram Int* 31: 1123–1130.

AIMS Press